Considerations of the effect of light interference on photon recycling via QFT

Jeffrey Morais[1, *]

[1] *Department of Physics, McGill University, Montreal, Canada*

We consider the logistics behind photon propulsion from continuously reflecting light in a semi-connected cavity payload, known as photon recycling. We investigate the effects of light interference on the radiation pressure by modelling light as a massless scalar field φ, and taking the interaction between light and the mirror to be a perturbative, coupled interaction in the Lagrangian density. We characterize the interference of light with an emphasis on a Feynman diagram approach with 1-loop diagrams and also look at other corrections to the radiation pressure arising from QFT such as the interaction of light at lowest loop level, and the static and dynamical Casimir effect. We consider the cases where the mirror boundary conditions are stationary and dynamic separately. It is found that compared to the macroscopic radiation pressure, the effects of the interference of light are suppressed by the prefactor with $\mathcal{O}(L^{-4})$, where L is the initial separation of the mirrors in the cavity. Moreover, we visualize this result for imperfect and perfectly reflecting mirrors over a range of reflectivities and initial cavity separations.

I. INTRODUCTION

The inefficiency of propulsion from combustion rockets leaves much to be desired when contemplating interstellar travel. An attractive alternative is the use of radiation pressure to accelerate payloads being made from reflective boundary conditions (BCs) such as light sails. Using directed radiation from a laser source to a light sail for example is inefficient as the energy conversion from the pressure to the spacecraft is inversely proportional to the spacecraft's velocity [1]. A potential fix to this problem is by having the light emitted from the laser reflect multiple times in a semi-connected resonant cavity or optical resonator. This is formed by reflective BCs, i.e., a partially transmitting mirror and a concave set of reflecting mirrors acting as the payload [2], which is known as photon recycling. This is visualized in Fig. 1. With every bounce the light imparts energy onto the mirror as it reflects off of in the form of momentum and redshifts accordingly, thus inducing propulsion on the payload. This process continues until all the energy is dissipated in the form of propulsion and gravitational energy due to the expansion of spacetime. The top and bottom mirrors of the payload do not contribute to the propulsion and neither does the radiation outside the semi-connected cavity, so we equivalently model the system as two mirrors initially separated by a distance L, with the gauge field propagating only within the two mirrors. Although the distance changes between the mirrors, for simplicity we refer to the two mirrors as the cavity of the system. One proposal considering photon recycling uses a fixed and unfixed mirror, treating photons as massless particles, and demonstrates theoretically with four-momentum conservation that a gram-scale spacecraft can be accelerated up to $0.2c$ [3]. The paper accounts for the Doppler shift when photons bounce back and impart energy, as well as the efficiency of said transfer but completely neglects the quantum nature of photons. This includes reflected photons interacting with incoming photons via loop-level interactions, interference, and the radiation emitted by a moving mirror in spacetime. Another consideration for photon propulsion uses a cavity with an internal boundary composed of highly reflective (HR) mirrors and demonstrates with optomechanics the possibility of accelerating the spacecraft. An interesting difference between the two papers is that the author of the latter claims that in a passive cavity composed of two HR mirrors, the incident and reflected beams of light within the cavity will interfere with each other destructively and resultingly impart negligible momentum onto the spacecraft [4]. Moreover, they suggest the fix to this is using an active gain medium in the optical cavity. The medium receives energy from an external source via laser pumping, and transfers part of its energy to the radiation as it passes through [5]. This is done through the stimulated emissions of photons as radiation imparts energy on confined electrons and they transition to a lower energy state. The author does not elaborate on this claim or show any theoretical computations to back it up. The different conclusions on from both approaches raises the main inquiry of interest in this paper: how much does interference between the incident and reflected beams affect the radiation pressure on the moving mirror? Being that the radiation pressure creates the propulsion of the mirror, the explicit computation of the effects of interference on the radiation pressure would naturally tell us how much the propulsion if affected. To answer this, we first focus on the case of stationary boundary conditions where the mirrors do not move, and compute contributions to the propulsion of the mirror from the radiation pressure and interference in the context of the Casimir effect. This approach is done using quantized scalar fields φ to describe light where the interaction between light and the mirror is modelled with perturbative coupled interaction vertices and Feynman diagrams. We then move on to the case where one mirror is moving relativistically and thus have a non-stationary boundary condition. We compute analogous contributions to the force exerted on the mir-

* jeffrey.morais@mail.mcgill.ca

ror, with the addition of radiation coming from moving mirrors in spacetime. This paper assumes knowledge of quantum field theory, statistical mechanics, and complex analysis. For a review of QFT and QED, the reader is recommended to look at chapter 2 and 4, respectively, of Peskin & Schroeder's textbook on QFT [6].

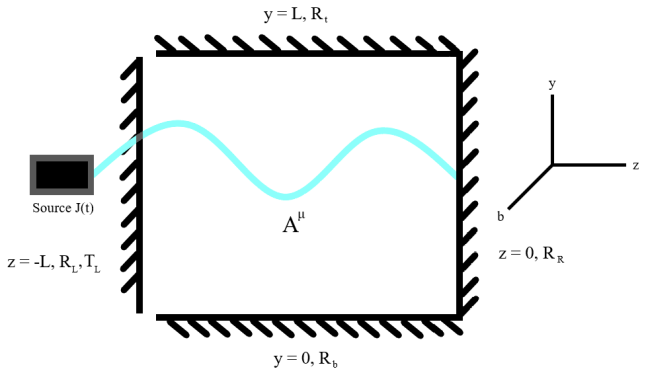

FIG. 1. Schematic of the semi-connected resonant cavity payload. Each mirror has an associated reflection coefficient, position, and if applicable, a transmittance coefficient. The laser source on the left $J(t)$ transmits light through the disconnected left mirror and reflects back and forth in the cavity to accelerate the cavity payload. Light is modelled as a gauge field A^μ.

II. STATIONARY BOUNDARY CONDITIONS

In this section we look at the different contributions or corrections that affect the radiation pressure, and hence propulsion, within the cavity formed by the mirrors with static BCs. This includes the radiation pressure from light within the cavity, the attractive Casimir force between the neutral plates, and the contributions from interference and scattering of light.

A. QFT & Massless Scalar Fields

Normally when dealing with radiation pressure and electromagnetic energy densities it is standard to use the principal U(1)-bundle in which case a Yang-Mills theory reduces to that of an electromagnetic theory, with the standard fiber being the complex line $\mathbb{C}$ for a local trivialization ϕ. The theory describes light in terms of oscillatory electromagnetic fields which is appropriate for describing systems with macroscopic separations and long wavelengths, however disregards quantum effects seen in quantum theory or QED. Moreover, when using such a description, there is no well-defined prescription when dealing with both the wave-like and particle-like nature of light simultaneously, which is the main discrepancy between the approaches for photon recycling reviewed in the introduction. To avoid these issues, we use a scalar field description of light where it is neither a wave nor a particle, it is rather a quantum object with certain properties and allowed interactions. This follows from the framework following the context of QFT, in which light is an excitation of a product vacuum Fock state $|0\rangle$. Moreover, the field theoretic approach is utilized to account for light interaction vertices not present in classical electrodynamics, as well as the fluctuation of quantum fields & the creation of particles from a relativistically moving mirrors in the Casimir and dynamical Casimir effect (DCE), respectively. This is important as at the length and energy scales where interference is considered, effects such as the DCE become relevant.

In QED, we describe fermions as spin-1/2 particles with spinor representations ψ and Grassmanian algebra, while photons are described as spin-1 bosons with vector/gauge field representations A_μ. The interaction between the two is encoded in the Lagrangian (omitting counter terms):

$$\mathcal{L} = \bar{\psi}(i\not{\partial} - m)\psi - \frac{1}{4}F_{\mu\nu}F^{\mu\nu} - e\bar{\psi}\not{A}\psi. \tag{1}$$

Here, m is the fermion mass, $F^{\mu\nu}$ are the components of the curvature 2-form, known as the field strength tensor, and e is the electron charge used as the coupling constant. The gauge field within the contraction $\not{A} = \gamma^\mu A_\mu$ is used as the connection in local coordinates $D_\mu = \partial_\mu + ieA_\mu$. For the purposes of the our analyses where the radiation pressure is incident on the parallel BCs, the polarization information within the gauge fields is not a concern. The case of the polarizations can be treated separately where they decouple and cancel the contributions of a mass correction from massless scalar fields [7]. We can alternatively treat the components of the gauge fields as massless scalar fields φ, and since we have two polarizations present in the spacetime components, we have two copies of the massless scalar fields. In this case, we can write the gauge field as the derivative of a scalar field $A_\mu = \partial_\mu\varphi$ and replacing the derivative with just the scalar field itself leaves us with Yukawa theory:

$$\mathcal{L} = \bar{\psi}(i\not{\partial} - m)\psi + \frac{1}{2}\partial_\mu\varphi\partial^\mu\varphi - g\bar{\psi}\psi\varphi. \tag{2}$$

This describes the interaction between spin-1/2 fermions and spin-0 scalar bosons. For the purposes of our analyses, we will only deal with the massless scalar fields to describe the radiation within the cavity φ and do not deal with fermions.

Moreover we note we will be working in natural units where $c = \hbar = k_B = 1$, and utilize the metric signature $\eta_{\mu\nu} = \mathrm{diag}(-1, 1, 1, 1)$.

B. Radiation Pressure From Scalar Fields

In this section we consider the radiation pressure on stationary, parallel boundary conditions (mirrors) using

quantized, massless scalar fields. One approach to this computation is the use of influence functionals described with path integrals [8]. In this approach, the mirrors are described with reduced density matrices with harmonic potentials centered on their potential, and the radiation is described with scalar fields that interact with the potentials via a perturbative, effective action term. They, however, do not deal with the case where the mirror moves a significant distance relativistically. Another approach quantizes the fluctuations of the scalar fields about a minimum such that it satisfies Dirichlet BCs, meaning it vanishes on the surfaces of the mirror, emulating the reflection properties of the mirrors. The perturbative action term acts as a description of the mirrors moving a differential amount and is used along with the BCs to derive an expression of the movement of the scalar fields. This is used to compute the amplitude of a motion induced energy density from the stress tensor in Euclidean space, and the radiation pressure is computed by taking the average over the field states [7]. Again, this is only for the case in which the mirrors move a differential amount in an oscillatory manner. Here, we briefly present a model for determining the photon pressure on the mirrors by considering the internal and mechanical degrees of freedom (DOF) of a moveable mirror in 1+1 D [9]. We then in later sections compare this result to change in pressure by interference affects it to see if it is significant.

The key property of a mirror is its reflective properties where the amplitude of the field vanishes at the boundary. The mirrors center of mass motion is treated like a massive particle of mass M with position coordinates $z(t)$ and the reflectivity is taken to be an internal DOF $q(t)$ which is modelled as a SHO of mass m and frequency Ω. This DOF is coupled to the field via the action functional:

$$\begin{aligned} S[\varphi,q] =& \frac{1}{2}\int d^2x\ \partial_\mu\varphi\partial^\mu\varphi\ + \int dt\Big[\ \frac{m}{2}(\dot{q}^2-\Omega^2q^2) \\ &+\ \lambda q\varphi(t,0)\Big]. \end{aligned} \tag{3}$$

Here λ is the renormalized coupling constant that is much smaller than unity to allow for perturbation theory. The associated EOM are found through varying the action and give:

$$\begin{aligned} -\partial_t^2\varphi+\partial_x^2\varphi &= \lambda q\delta(x) \\ m\ddot{q}+m\Omega^2q &= \lambda\varphi(t,0). \end{aligned} \tag{4}$$

Now, consider the cavity formed by these two mirrors with one fixed and one moving (although this section considers stationary BCs, we are in the limit where $\delta z(t) \ll L$) with the perfect reflection condition being the Dirichlet BC $\varphi(t,0)=0$. We take the reflectivity of the second mirror only to be partial, thus allowing for the presence of an external source $J(x^\mu;\Omega_D) = A\cos\Omega_D t$, where the frequency of the external pump is Ω_D. The Lagrangian for such a system is of the form:

$$\begin{aligned} \mathcal{L} =& \frac{1}{2}[\partial_\mu\varphi\partial^\mu\varphi + 2J(x^\mu)\varphi + m(\dot{q}^2-\Omega^2q^2) \\ &+ M(\dot{z}^2-{\Omega_0}^2z^2) + 2\lambda q\varphi(t,L+z(t))]. \end{aligned} \tag{5}$$

Using coordinates $x = L + z(t)$ and the fact that the mirror moves through a harmonic potential of natural frequency Ω_0, we have the associated EOM:

$$\begin{aligned} -\partial_t^2\varphi+\partial_x^2\varphi &= J(x^\mu)+\lambda q\delta(x-L-z(t)) \\ \ddot{q}+\Omega^2q &= \frac{\lambda}{m}\varphi(t,L+z(t)) \\ \ddot{z}+\Omega_0^2z &= \frac{\lambda}{M}q\partial_x\varphi(t,L+z). \end{aligned} \tag{6}$$

From these EOM, the differential equation for z(t) can be isolated and modelled as a damped, forced harmonic oscillator. We can then consider the mirror cooling with motion in the weak interaction limit $\lambda^2/(m\Omega^3) \ll 1$, as well as the geometric condition $\Omega, \Omega_D \gg \Omega_0$. This allows us to then time average over the mirror's EOM and get:

$$M\ddot{z}+\Gamma(L)\dot{z}+M(\Omega_0^2-\delta\Omega^2(L))z = F(L), \tag{7}$$

where Γ is the damping coefficient, $F(L)$ is the radiation pressure, and $\delta\Omega$ is the frequency shift. The explicit form of the radiation pressure is given by:

$$F(L) = \lambda^2\alpha\tilde{D}(\Omega_D)(\alpha'^* + \frac{\lambda^2}{2}\alpha^*\tilde{D}^*(\Omega_D)\mathrm{e}^{-i2\Omega_D L}). \tag{8}$$

Here $\alpha = A(\mathrm{e}^{i\Omega_D L}-1)/2\Omega_D^2$, $\alpha' = \partial_{\Omega_D}\alpha$ are oscillatory functions, and $\tilde{D}(\Omega_D)$ is the Fourier transform of the kernel of the DOF $q(t)$:

$$\tilde{D}(\Omega_D) = \frac{\Omega_D}{2m\Omega_D({\Omega_D}^2-\Omega^2)+i\lambda^2(1-\mathrm{e}^{2i\Omega_D L})}. \tag{9}$$

The expression for the radiation pressure in the cavity of the perturbed mirror will be a source of interest when comparing the order of magnitude to the force fluctuation due to interference, covered in the next section.

C. Casimir Effect & Interference

The fluctuation of scalar fields gives rise to a force on macroscopic boundaries, such as the Casimir force for neutral, parallel, metal plates in a vacuum. In this section, we look at the derivation of the force using Feynman diagrams to develop an intuition of how interference affects the pressure.

Consider a massless scalar field theory with a quadratic spatially dependent interaction of the form $\mu^2\varphi^2\theta(z)$. The Lagrangian density has the form:

$$\mathcal{L} = \frac{1}{2}\partial_\mu\varphi\partial^\mu\varphi - \mu^2\varphi^2\theta(z), \tag{10}$$

where the spatial function coupled to the interaction has the form $\theta(z) = -i\int dk_z \frac{e^{ik_z z}}{k_z - i\varepsilon}$. We note that due to our convention for the metric, the usual signs of the imaginary units in the propagator are flipped to adhere to the $i\varepsilon$ prescription. This gives rise to an interaction vertex of the form:

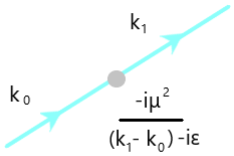

FIG. 2. Quadratic interaction vertex (gray dot) with a single momentum coming in and going out. The contribution of this vertex is shown in the image.

Now, consider a slab of metal centered at $z = 0$ extending to infinity in the xy plane. For $z < 0$, we say the field is massless, while for $z > 0$, the interaction modifies its dispersion relation. Consider a field φ coming in from the right with momentum k_0 and at some height above exits the mirror with momentum k'. Note that the height of the field does not actually increase, this is just to visualize the reflection. In $z > 0$, the paths are connected by various interaction vertices. The full path propagating from the left, connecting to interaction vertices and leaving towards the left will be our description of the field reflecting off the mirror:

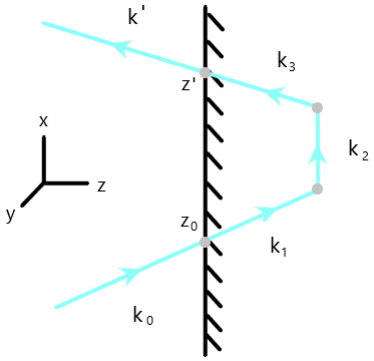

FIG. 3. Feynman diagram of photons reflecting off of a mirror centered at $z = 0$, described with connected interaction vertices on the right side of the mirror.

At each vertex, only $k_\perp$ along the $\hat{x}$-direction is conserved and not k_z, as we can have such connected paths that change direction instantly which clearly do not conserve momentum along the $\hat{z}$-direction. This means that all the momenta connecting the interaction vertices for $z > 0$ are undetermined and are integrated over. We write down the amplitude for this diagram using Feynman rules analogous to φ^4 theory:

$$\begin{aligned} iM =& \frac{1}{\bar{S}}\int \frac{d^2k_1 d^2k_2 d^2k_3}{(2\pi)^8} \frac{-i\mu^2}{(k_1 - k_0) - i\varepsilon} \frac{i}{k_1^2 - \omega_1^2 - i\varepsilon} \\ &\times \frac{-i\mu^2}{(k_2 - k_1) - i\varepsilon} \frac{i}{k_2^2 - \omega_2^2 - i\varepsilon} \frac{-i\mu^2}{(k_3 - k_2) - i\varepsilon} \\ &\times \frac{i}{k_3^2 - \omega_3^2 - i\varepsilon} \frac{-i\mu^2}{(k' - k_3) - i\varepsilon} e^{i(k_0 z_0 - k' z')}. \end{aligned} \tag{11}$$

Here $\bar{S}$ is the symmetry factor of the diagram. We proceed with external leg amputation to avoid tree-level divergences for external lines in $z < 0$ and take all momenta in $z > 0$ to be on shell. This gets rid of the exponential term at the end of the diagram amplitude.

Now, we can compute the integrals with Feynman parameterization but we instead make use of residue theorem:

$$\oint_\gamma dz f(z) = 2i\pi \sum_k \mathrm{Res}(f, z_k). \tag{12}$$

We first look at the k_1 complex plane, and note that there are fewer poles in the upper half of the complex plane so we close the contour in the upper half of the complex plane with a semicircular contour. The poles are depicted in the following figure:

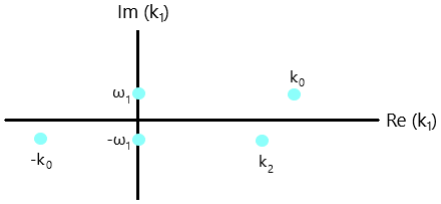

FIG. 4. Complex k_1 plane with the corresponding poles of the diagram's amplitude represented by blue dots.

One of the residues for example has the form:

$$\begin{aligned} \mathrm{Res} f(k_0) =& \partial_{k_1}\left[\frac{1}{(k_1 + k_0 - i\varepsilon)(k_2 - k1 - i\epsilon)}\right]\Bigg|_{k_1 = k_0} \\ \sim& \frac{1}{(k_0 - k_2)k_0}. \end{aligned} \tag{13}$$

It follows from Jordan's lemma that the function parametrized to the semi-circle of radius R vanishes as

$R \to \infty$, so we are just left with integration over the real line. Repeating this for all poles within the contour, we end up with a function of the form:

$$iM = \frac{1}{2k_z} f\left(\frac{\mu^2}{k_z^2}\right). \tag{14}$$

Note: $f\left(\frac{\mu^2}{k_z^2}\right)$ is the exact form of the reflection coefficient R, so the diagram contribution is the reflectivity of the mirror.

Now consider two mirrors spatially separated along the z-axis. The Lagrangian density now takes the form:

$$\mathcal{L} = \frac{1}{2}\partial_\mu\varphi\partial^\mu\varphi - \varphi^2[\mu_L^2\theta_L(z) + \mu_R^2\theta_R(z)]. \tag{15}$$

The diagram is depicted in the following figure:

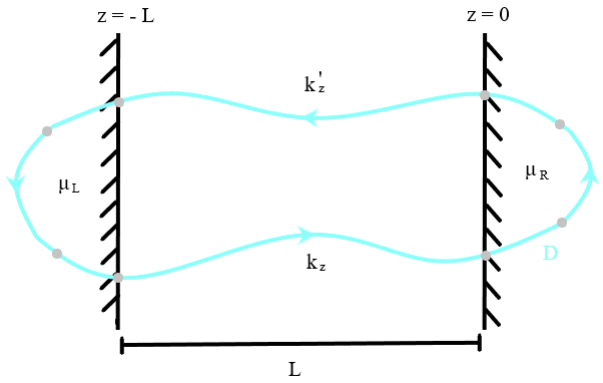

FIG. 5. Feynman diagram of light bouncing off both mirrors, represented with interaction vertices outside the mirrors. The length of the cavity that the mirrors form is L. The Feynman diagram going through both mirrors (in blue) is referred to as the diagram D.

We would like to compute the vacuum energy between the plates to recover the force, without the contribution of the mirror's individual self-energies. This is done under the temporal-spatial limit $L, T \to \infty$ for the vacuum energy ε:

$$\varepsilon = \lim_{L,T\to\infty} -\frac{1}{LT}\log Z, \quad Z = \int \mathcal{D}\varphi e^{-S[\varphi]}. \tag{16}$$

Here, Z is the continuous limit of the partition function in Euclidean space. We can relate it to the $Z[J]$ functional for interacting theories in QFT by first applying a Wick rotation to be in imaginary time, and then adding an additional term to the interacting Lagrangian in the form of an external source J:

$$Z \to \oint \mathcal{D}\varphi e^{iS[\varphi]} \to Z[J] = \int \mathcal{D}\varphi e^{i\int d^4z[\mathcal{L}_0 + J\varphi]}. \tag{17}$$

Now, a general diagram D is composed of many interior connected diagrams C_i. We can write D as $D = \prod_i \frac{C^{n_i}}{n_i!}$, where n_i counts the number of times C_i appears in D, and $\frac{1}{n_i!}$ is the symmetry factor corresponding to the connected diagrams C_i. We can express $Z[J]$ as the sum of all general diagrams D:

$$\begin{aligned} Z[J] \propto \sum_{\{n_i\}} D = \sum_{\{n_i\}} \left(\prod_i \frac{C^{n_i}}{n_i!}\right) = \prod_i \sum_{\{n_i\}} \frac{C^{n_i}}{n_i!} \\ = \prod_i \exp(C_i) = \exp\left(\sum_i C_i\right). \end{aligned} \tag{18}$$

We see that Z is the exponential of the sum of all connected diagrams, so $\log Z$ in ε takes the amplitudes of the connected diagrams and kills off any disconnected diagrams. We denote the two mirror diagram D, which is composed of various connected diagrams with the interaction vertex.

Now for a single diagram D with N interaction vertices, we can rotate it N different ways and leave it invariant so the symmetry factor is $\bar{S} = N$:

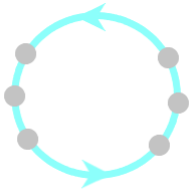

FIG. 6. Feynman diagram going through both mirrors, diagram D, represented in a simpler form of just a circle. The N interaction vertices are visualized with grey dots. The idea is that rotating this diagram leaves it invariant so there is a symmetry factor associated with it.

For a pair of two D diagrams, we can swap them and leave the amplitude invariant so the symmetry factor is $\bar{S} = 2$:

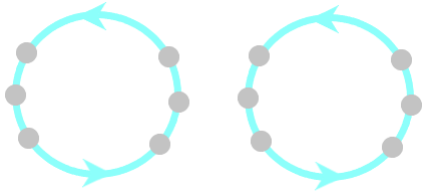

FIG. 7. A set of two D diagrams that are invariant under swapping the individual D diagrams. This means it has an associated symmetry factor.

We can expand $\log Z$ in terms of the D diagrams as:

$$\log Z \sim 1 + \frac{d_1}{N}D + \frac{(d_2)^2}{2N}D^2 + \dots \tag{19}$$

Here D^j refers to j D-diagrams, so the case we saw before with two corresponds to D^2. Moreover, d_j are simply real coefficients in the expansion. If we sum up all the contributions of the diagrams, in the temporal-spatial limit, only the diagram D survives. Now, looking at the figure for the two mirror diagram, we take the contributions of μ_L, μ_R, the two propagators and external legs, we get:

$$iM \sim \int \frac{dk'_z}{2\pi}\frac{dk_z}{2\pi}\frac{dk_x dk_y d\omega_E}{(2\pi)^3}\frac{\mu_L\mu_R e^{iL(kz-k'z)}}{(k_z^2+k_x^2+k_y^2+\omega_e^2)} \times \frac{1}{(k'^2_z+k_x^2+k_y^2+\omega_e^2)}. \tag{20}$$

After computing the residues, it follows:

$$iM \sim \int \frac{d_k x dk_z d\omega_E}{(2\pi)^3}\frac{\mu_L}{2k_z}\frac{\mu_R}{2k_z}e^{-2L\sqrt{k_x^2+k_y^2+\omega_e^2}} = \int \frac{d^3k}{(2\pi)^3}R_L R_R e^{-2L\sqrt{k^2}}. \tag{21}$$

Here $k^2 = k^\mu k_\mu = -k_0^2+\vec{k}^2$. From this we get the energy by computing the integration in spherical coordinates. We then recover the force by taking the negative spatial gradient with respect to the initial length of the cavity. This gives the following expression:

$$F(L) = -\frac{3R_R R_L}{16\pi^2 L^4}. \tag{22}$$

Note the negative sign in front tells us that this force is attractive between the mirrors in the cavity. This represents the contribution of the force without the effects of interference.

Now, we must consider the many reflections that occur between the mirrors and characterize the interference of the photons as a multiple scattering series. An example of such a reflection diagram is:

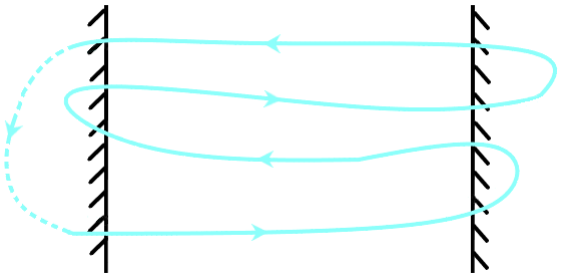

FIG. 8. Feynman diagram of interference, represented by light bouncing back and forth between mirrors.

It follows that our original two mirror D diagram is the first term in the scattering series, and we also have for example diagrams corresponding to 3 and 6 , respectively:

FIG. 9. Feynman diagrams representing three and six reflections off of the mirrors, respectively.

For example, looking at the three reflection diagram, we see two nodes on the right. These nodes can be cyclically swapped without the amplitude changing, so we associate a symmetry factor of $\bar{S} = 2$. In general, for every n nodes corresponding to $2n$ reflections, the reflection diagram has a symmetry factor of $\bar{S} = n$. We may now write all of the new contributions to $\log Z$ in terms of the reflection diagrams:

$$\log Z \to \frac{1}{2}\int_{\omega,k_x,k_y} R_L R_R e^{L\sqrt{\cdots}} + \frac{1}{2\cdot 2}\int_{\omega,k_x,k_y}(\ )^2 + \frac{1}{2\cdot 3}\int_{\omega,k_x,k_y}(\ )^3 + \ \ldots \tag{23}$$

We see that the effect of interference changes the original integrand to log (1- integrand). Finally, now that we have our full expression for $\log Z$, we compute the force by differentiating the energy with respect to the distance between the mirrors:

$$F(L) = -\frac{d\varepsilon}{dL} = -\frac{1}{2}\int \frac{d}{dL}\log(1 - R_R R_L e^{-2L\sqrt{k^2}}). \tag{24}$$

This is the Lifshitz formula for the Casimir force between two mirrors in a vacuum. For perfectly reflecting mirrors such that $R_j = -1$, then the energy and force per unit area reduces to:

$$\varepsilon = -\frac{\pi}{1440L^3} \implies F(L) = -\frac{\pi^2}{480L^4}. \tag{25}$$

This gives us our desired result of how interference affects the force on mirrors by the interference of the radiation pressure. This is seen between the two expressions for the contributions of the force, Eq. 22, and Eq. 25. We see the only difference is a slight increase in the prefactor from ~ 0.019 to ~ 0.021. Moreover, we see compared to the macroscopic force of the radiation pressure on the mirrors given by Eq. 8, the effect of interference is negligible. Eq 25 is in accordance with the Casimir effect derived in 4 dimensional Minkowski spacetime [10]. Note, the inclusion of the two polarizations of light results in a factor of two, as computed by the paper cited in the line above. The force is visualized in the following plot:

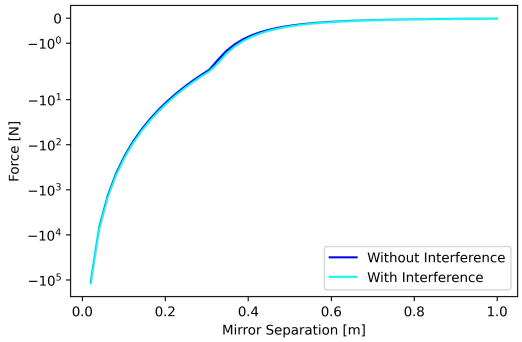

FIG. 10. Plot of the Casimir force with and without interference as a function of the initial separation of the mirrors forming the cavity. The vertical axis is using a logarithmic scale to emphasize the divergent feature at no separation. We note that the anomalous change in curvature at $L \sim 0.3$ is an artefact generated by the `symlog` function in Python used to logarithmically scale negative-values in the vertical axis, and has no physical meaning. We see that it is only significant at small separations of the mirrors.

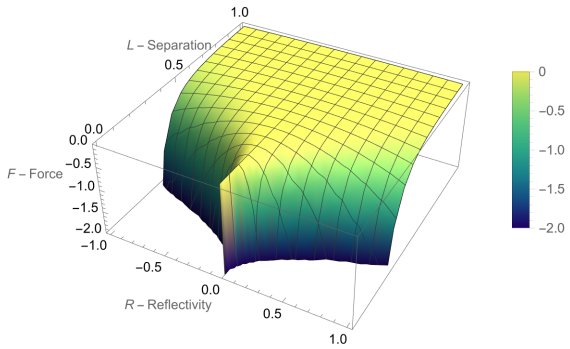

FIG. 11. Plot of the Casimir force between two mirrors as a function of the initial separation, and different reflectivities of the mirrors. The cusp shape near the completely absorbent point comes from the square root dependence of the reflectivity in the argument of the integrated exponential.

Note: We have only considered stationary mirrors. In the next section, we look at the dynamical Casimir effect for moving boundaries.

We can also consider the case in which the mirrors are not necessarily perfectly reflecting in the case where interference is included. To visualize this in 3 dimensions, we consider both mirrors to have the same reflectivity $R_R = R_L = R$, which results in the following expression for the attractive force:

$$F(L,R) = -\frac{3\,\mathrm{Li}_4(R^2)}{16\pi^2 L^4}, \tag{26}$$

where $\mathrm{Li}_n(z)$ is the polylogarithm function for a complex argument z with power n. We plot the Casimir force for reflectivities ranging from completely transparent $R = 1$, to completely absorbent $R = 0$, and to completely reflecting $R = -1$. This is visualized in the following plot:

Finally, the presence of a medium gain with transmittance T would simply change the contributions of the external legs for the final expression of the force:

$$\mathrm{e}^{-kL} \to \mathrm{e}^{-kL+T\beta}, \quad \beta \in \mathbb{C}. \tag{27}$$

The result of the force agrees with an alternative approach that utilizes the Gelfand-Yaglom theorem for functional determinants [11]. Refer to the appendix for a brief overview of the approach.

D. More On Interference

In the previous section we saw the contribution of reflection and the interference of photons on the force between two neutral, parallel, metal plates interacting with a massless scalar field. This leads to a series of reflections which produced a log(1-integrand) term in the new integrand. It should be noted that a caveat for this approach is that the calculations are done in real time with the partition functional Z. This means that the exponential terms instead of being phases of complex vectors that can interference with each other in imaginary time, we have the multiplications of numbers which in itself is not interference. The diagram calculations, however, are done in imaginary time with the use of a Wick rotation.

Usually interference of photons in considered within the case of Young's experiments or beam splitters, typically described via path integrals or Fock states within a defined Hilbert space with quantum fields [12]. During an extensive literature review, an interesting claim was found describing the interpretation of the Lorentz radiation pressure force on submerged mirrors [13]. In it they consider mirrors with Fresnel reflection coefficients with phase angles ϕ_0 submerged in a dielectric (in our case the vacuum can be thought of a dielectric via vacuum polarization) with refraction index n. Within the

region of the liquid that is within the cavity formed by the two mirrors, the incident beam interferes with the reflected beam as expected. The claim is that the resulting Lorentz force that the interference fringes exert on the liquid pulls away from the mirror given a phase angle $\phi_0 = \pi$, and pushes towards the mirror for $\phi_0 = 2\pi m$, where $m \in \mathbb{Z}$. They conclude the contribution of interference to be negligible and that the total force acting both on the mirror and the liquid is the same regardless of the value of the phase angle ϕ_0.

E. Photon Scattering

When photons bounce off the mirror they will interact with one another via the perturbative interaction term given in Yukawa theory as covered in the first section when working within our approximation that we model photons with massless scalar fields. For the following consideration we work in the framework of QED with gauge fields A_μ for photons. At first loop order, photons interact via the following diagram:

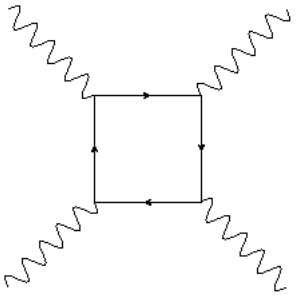

FIG. 12. Photons interacting with each other at first loop order via a virtual fermion loop.

For example, the probability of two photons coming in both with positive polarization and exiting with both negative polarization is computed for the diagram above and is given by [14]:

$$|iM_{++--}|^2 = \left| -\frac{11\alpha^2 s^2}{45m^4} \right|^2 , \tag{28}$$

where α is the fine structure constant, $s = (k_1+k_2) = 4\mathrm{e}^2$ is the usual Mandelstam variable, and m is the renormalized electron mass. We see that the probability is fairly suppressed and will not affect the photon pressure force on the mirrors by a significant amount. Moreover, there are 3-loop order contributions to the interaction, but it does not raise the probability significantly:

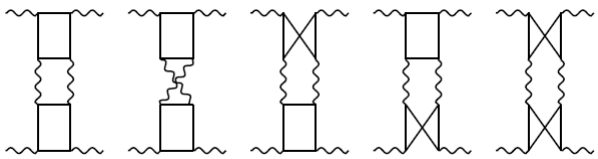

FIG. 13. Photons interacting at third loop order via multiple virtual fermion and virtual fermion/photon loops [15] .

III. DYNAMIC BOUNDARY CONDITIONS

In this section we consider the right boundary condition (mirror) to be in motion, either perturbatively or relativistically along a worldline $x = z(t)$ in 1+1 D spacetime dimensions, where t is an affine parameter. Once more we look at how the radiation within the cavity exerts a pressure on the mirrors and the effects of the interference of light. Due to the motion of the mirror, we also run into the creation of particles and radiation due to the dynamical Casimir effect (DCE).

A. Radiation Pressure From Quantized Fields

In this section, we look at analysis done for computing the radiation pressure of massless scalar fields on moving mirrors with Dirichlet or Robin BCs [16]. Once again we consider a field $\varphi(t, x)$ obeying the massless Klein Gordon (KG) equation for a BC moving relativistically with coordinates $z(t) \equiv x$. In the rest frame of the lab, one can write the vanishing Dirichlet/Robin BCs after applying the appropriate representations of the Poincaré group as:

$$\varphi(t, z(t)) = 0, \;\; [\dot{z}\partial_t + \partial_x]\varphi(t, x)|_{x=z(t)} = 0. \tag{29}$$

One can use the conformal (transformation) invariance of the KG to obtain the lab frame solution with the transformations: $t - x = f(\omega - s)$ & $t + x = g(\omega + s)$. This gives rise to the BCs taking a simpler form:

$$\varphi(\omega, o) = 0, \;\; \partial_s\varphi(\omega, s)|_{s=0} = 0. \tag{30}$$

We have the usual expansion of the scalar field φ in terms of quantized annihilation and creation operators, a and $a^\dagger$, respectively, and the associated eigenfunctions:

$$\varphi_\omega(t, x) = \frac{1}{\sqrt{4\pi\omega}} \left(\gamma \mathrm{e}^{-i\omega\pi r(v)} + \gamma^* \mathrm{e}^{-i\omega\pi p(u)} \right). \tag{31}$$

Here $u = t-x$, $v = t+x$, $\gamma = 1, i$ for Robin and Dirichlet BCs, respectively. If we consider a light cone within the ambient spacetime centered at the origin, the positive and negative positions are denoted by regions i and iv, respectively, and for the positive temporal regions, and

those to the left of it within the light cone (the retarded trajectory of the mirror)as ii and iii, respectively. This is visualized in the following figure:

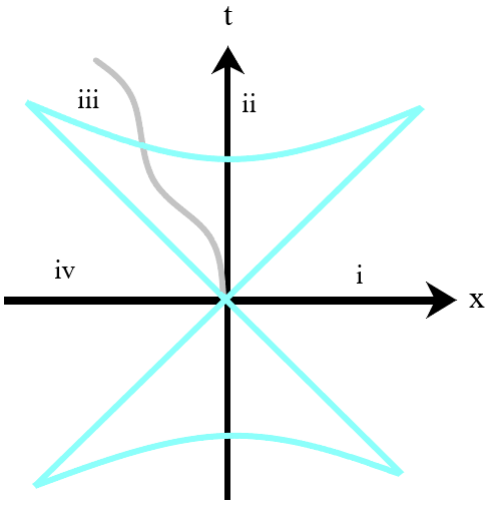

FIG. 14. Light cone centered at origin, with various regions marked. The gray trajectory represents the motion of the mirror before passing to positive values of displacement.

For regions i & ii it follows that $r(v) = v, p(u)$, and $2\tau(u) - u = f^{-1}(u)$, where $\tau(u)$ is implicitly solved from $\tau(u) - z\,[\tau(u)] = u = p(u)$. For regions iii and iv, it follows that $p(u) = u$, and $2\tau(v) - v = g^{-1}(u) = r(v)$.

The force on the moving boundary can then be found by averaging over the first component of the stress tensor $\bar{T} = \langle T_{oo}(t,x)\rangle$ and adding up the contributions from regions iii & iv, and i & ii respectively, denoted (-) and (+):

$$F(t,x) = \bar{T}(t,x)^{(-)} + \bar{T}(t,x)^{(+)}. \tag{32}$$

Of the total force experienced by the mirror, the contribution from the radiation pressure can be expressed as:

$$F = 2\int d\omega d\omega' \langle a^\dagger_{\omega'} a_\omega\rangle \Lambda(\omega,\omega',\gamma^*,\gamma), \tag{33}$$

where Λ has the functional form:

$$\begin{aligned}\Lambda(\omega,\omega',\rho,\lambda) =& \frac{\sqrt{\omega\omega'}}{4\pi}\Big[-\rho^2\left(\frac{1+\dot{z}}{1-\dot{z}}\right)^2 \mathrm{e}^{-i(\omega-\omega')p[t-z(t)]} \\ &+ \rho^2 \mathrm{e}^{-i(\omega-\omega')[t-z(t)]} \\ &- [(z,\dot{z},p,\rho)\to(-z,-\dot{z},r,\lambda)]\Big].\end{aligned} \tag{34}$$

Here the last term in the expression above with the arrow indicates repeating the same component as before except with the parameters within the argument swapped.

Finally, to get an explicit expression for the integral above, consider a thermal bath of a finite temperature T that is invariant under time-translations, meaning that $\langle a^\dagger_{\omega'}, a_\omega\rangle = 1/(\mathrm{e}^{\omega/T} - 1)\delta(\omega' - \omega)$. This results in the radiation pressure force on the moving mirror as the following:

$$F(\dot{z}) = -\sigma_T\left[\dot{z}\left(\frac{1+\dot{z}}{1-\dot{z}}\right)^2\right]. \tag{35}$$

Here $\sigma_T = 2|\gamma|^2\pi T^2/3$ is the viscosity coefficient. The expression above will be compared to the force difference from the effects of interference.

B. Dynamical Casimir Effect

With accelerating, relativistic, moving boundary conditions, we have the production of particles and energy densities in the form of radiation [17], known as the dynamical Casimir effect (DCE). Within the context of QFT in curved spacetime, analogous analyses are used to describe Hawking radiation and the Unruh effect.

1. *Optomechanical Cavity Approach*

One way to describe the dynamical Casimir effect is having a resonant cavity made of mirrors with one boundary connected to a spring. The oscillatory motion of the mirror squeezes the cavity non-adiabatically thus inducing fluctuations of the fields and the production of particles from the vacuum. The effect is modelled as a scattering process that converts phonons (a collective excitation in a periodic and elastic arrangement of atoms, in this case the mirror attached to the spring) to photons [18].

The motion of the mirror is perturbative, non-relativistic, and has the following Hamiltonian:

$$H = \omega_c a^\dagger a + \omega_m b^\dagger b + V. \tag{36}$$

Here ω_c is the frequency of the cavity field operator $a^\dagger$, ω_m is the frequency of the SHO spring motion, and $b^\dagger$ is the SHO field operator. The radiation pressure on the mirror has an operator that can be expressed as:

$$F = \frac{\omega_c}{2L}\left(a + a^\dagger\right)^2. \tag{37}$$

With this, we write the interaction term as $F = Vx$, where x is written as usual in terms of the $b^\dagger$ operators to give the interaction term:

$$V = Fx = g a^\dagger a\left(b + b^\dagger\right) + \frac{g}{2}\left(a^2 + a^{\dagger 2}\right)\left(b + b^\dagger\right). \tag{38}$$

This gives rise to two types of interaction vertices: optomechanical vertices for the SHO and dynamical Casimir vertices for the cavity, with associated Feynman rules. This can be used to compute dressing effects such as corrections to the oscillator and cavity frequencies using associated one particle irreducible (1PI) diagrams, the renormalization of the field strength, and the correction to the ground state energy.

For the purposes of the radiation pressure from the dynamical Casimir effect, diagrams in which phonons are converted into two photons (artefact at tree level) are considered, due to the fact that the DCE is essentially energy transferring from the mirror to the field. When photons are generated from the vacuum, they take energy from the mirror and exert radiation pressure on the boundary, known as the backaction effect. To compute the force, you take the interacting vacuum expectation value of the force operator introduced before, using the usual form of the expectation value:

$$\langle\Omega|T[A(t_1)B(t_2)]|\Omega\rangle = \langle 0|U_I(\infty,-\infty)|0\rangle^{-1}\times \\ \langle 0|T[U_I(\infty,t_1)A_I(t_1)U_I(t_1,t_2)B_I(t_2)U_I(t_2,-\infty)]|0\rangle. \tag{39}$$

Here, T is the time-ordering operator, $A(t), B(t)$ are time dependent operators, and $U_I(t)$ is the unitary evolution operator in the interacting picture. Taking A and B to be the backaction force at different times, the correlation function for the force observable at different times is computed:

$$\langle\Omega|T\left[F(t_1)F(t_2)\right]\Omega\rangle = \frac{\omega_c^2}{AL^2}\mathrm{e}^{-2i\omega_c(t_1-t_2)}. \tag{40}$$

It is seen that the backaction force at different times has non-vanishing correlations at $\mathcal{O}(L^{-3})$, which is a very small number macroscopically when compared to the radiation pressure in Eq. 35.

2. *Iterative Diagram Approach*

Now we are interested in the case of a non-perturbative, relativistic motion of the boundary condition. We take an iterative approach, similar to how the Casimir force with interference was derived in the static BCs section. First, consider the fact that a highly reflective material has a very small penetration depth, so light spends very little time within the mirror before it reflects off. This means that the mirror only accelerates over a small time interval for each reflection and thus we can approximate that its motion is uniform during so. This means that the mirrors velocity is modelled by discontinuous, instantaneous increases after every reflection off the moving mirror, like an increasing step function. For clarity, whenever we mention a moving mirror, it refers to the one on the right of the cavity, meaning the one on the left is fixed and always stationary. Moreover, it is worth noting that relativistic effects such as time dilation and length contraction do not appear here as we are only interested in the time elapsed in the lab frame where the mirror is in motion, and length contraction would only apply to the thickness of the mirror which does not affect calculations. Thus the only relativistic effects present is the redshifting of light after each reflection.

We take the origin to be centered at the moving mirror's initial position, and take the first time step t_1 to be the time when light first comes in contact with the moving mirror. This imparts momentum on the mirror, and the next time step is when light hits the left stationary mirror. The next time step occurs when light hits the moving mirror again. This is then repeated for $N/3$ reflections. This is visualized in the following figure:

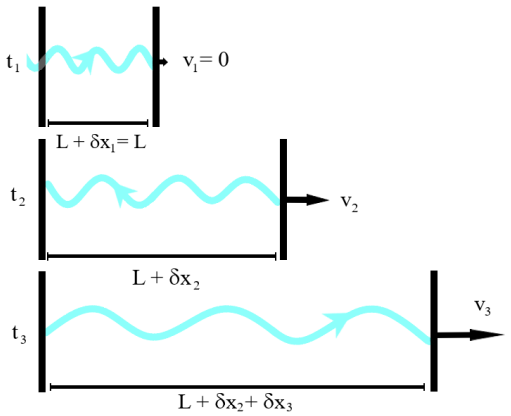

FIG. 15. Setup of photon recycling. Light transmits through the left mirror and reaches the right mirror at t_1, where the moving mirror has been displaced by $\delta x_1 = 0$. Light then reflects off the mirror, imparting momentum onto the right mirror with velocity v_2 and redshifting accordingly. Light reaches the left mirror at $t = t_1 + t_2$ and the process of reflecting and redshifting continues until the light has negligible energy.

Although we have labelled them differently to find the recursion relation, the velocity of the mirror only changes after every two time steps so we say $v_{2i} = v_{2i+1}$ where i refers to the ith reflection, and $i = 1$ is when light firsts hits the right mirror, and $i = 2$ is when it first hits the left mirror. Moreover, after a reflection off the right mirror, although the mirror gains momentum, the distance between the light and the left mirror has not changed, so we say $t_{2i-1} = t_{2i}$. Using these two conditions, we can recursively find the displacement of the mirror for the ith reflection, as well as the time spent during the displacement:

$$\delta x_i = v_i\, L \prod_{j=1}^{\lfloor \frac{i-1}{2} \rfloor} \left(\frac{1+v_{2j}}{1-v_{2j}}\right), \quad \delta t_i = \left(\frac{\delta x}{v}\right)_i. \tag{41}$$

We thus have the size of the cavity at the N-th reflec-

tion given by $L_N = L + \sum_{i=1}^{N} \delta x_i$ which will be useful when considering the force on the mirror. Now, the initial conditions we have is that the mirror is initially at rest $v_1 = 0$ and the momenta of the photon first coming in is fixed to k_1, but what are the subsequent velocities of the mirror and red-shifted momenta of the photon? To do this, consider radiation hitting a moving mirror, expressed by the i) partition of the following diagram:

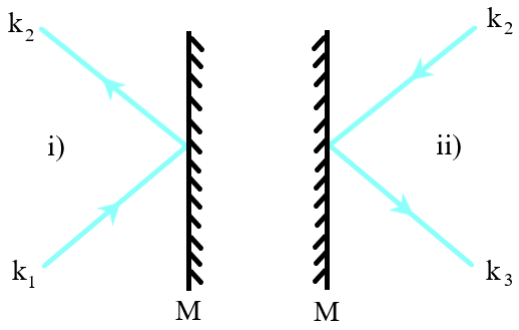

FIG. 16. Light reflecting off a mirror. i) Light reflecting off the right moving mirror and redshifting after reflecting. ii) Light reflecting off the fixed, stationary left mirror and not redshifting after reflection.

We can write the four momenta before and after the reflection event, given by the following:

$$\begin{aligned} p^{\mu}_{\gamma,1} = (k_1, k_1), \;\; p^{\mu}_{M,1} = (E_1, \gamma_1 M v_1) \\ p^{\mu}_{\gamma,2} = (k_2, -k_2), \;\; p^{\mu}_{M,2} = (E_2, \gamma_1 M v_2). \end{aligned} \tag{42}$$

Here $\gamma_j = [1 - v_j^2]^{-\frac{1}{2}}$ is the usual Lorentz factor. From this we can write down momentum and energy conservation, respectively:

$$\begin{aligned} \gamma_1 M v_1 + k_1 = -k_2 + \gamma_2 M v_2 \\ k_1 + M\sqrt{1 + \gamma_1^2 v_1^2} = k_2 + M\sqrt{1 + \gamma_2^2 v_2^2}. \end{aligned} \tag{43}$$

Finally, we consider adding the two equations and subtracting the first equation from the second, respectively. Moreover, we replace the $1, 2$ subscripts with $i, i' = i + 1$ for the sake of setting up a recursion relation. These two equations are given by:

$$\begin{aligned} 2k_i + M(\gamma_i v_i + \sqrt{1 + \gamma_i^2 v_i^2}) = M(\gamma_{i'} v_{i'} + \sqrt{1 + \gamma_{i'}^2 v_{i'}^2}) \\ M(\sqrt{1 + \gamma_i^2 v_i^2} - \gamma_i v_i) = 2k_{i'} + M(\sqrt{1 + \gamma_{i'}^2 v_{i'}^2} - \gamma_{i'} v_{i'}). \end{aligned} \tag{44}$$

From the first equation we can in principle isolate for the velocity of the mirror after reflection to be a function of the initial light momentum k_i, the initial velocity of the mirror v_i, and the mass of the mirror M, to get $v_{i+1} = f(v_i, k_i; M)$. Solving this analytically, however, fairs very poorly for computation time and convergence (as attempted in a Mathematica notebook) for N reflections. Instead, when computing for the velocity of the mirror after the ith reflection, we begin with the initial condition $v_1 = 0$, plug that in to get an equation with numbers and numerically repeat the iterations for N reflections.

Moreover, for the second equation we could also in principle solve for the new momentum of the red-shifted light as a function of the mirror velocities before and after the event, photon momentum, and mirror mass to get $k_{i+1} = \tilde{g}(v_i, v_{i+1}; M) = g(v_i, k_i; M)$, where $g = \tilde{g} \circ f$, and f is the velocity function as described before. However, again we run into convergence time issues and proceed with a numerical propagation of computations, given a fixed initial $k_1 \neq 0$ momentum for the photon.

We can also consider the case in which light reflects off the left fixed mirror, as seen in Fig. 16 ii), whose four momenta are given by:

$$\begin{aligned} p^{\mu}_{\gamma,2} = (k_2, -k_2), \;\; p^{\mu}_{M} = (M, 0) \\ p^{\mu}_{\gamma,3} = (k_3, k_3), \;\; p^{\mu}_{M} = (M, 0). \end{aligned} \tag{45}$$

Note we do not include subscripts on the different 4 momenta of the fixed mirror as it does not gain energy. We see from this that light does not get red-shifted as it reflects off the mirror and thus has the same momenta. This will be useful when considering loop diagrams for moving mirrors.

Now that we have the expression for the cavity size, the velocities of the mirror and the red-shifted momenta of the light within the cavity, we move on to generalize our results in the static boundary condition section by considering diagrams with a moving mirror. Consider first the case where light reflects off both mirrors once, visualized in the following figure:

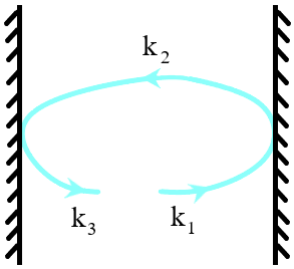

FIG. 17. Light reflecting off of both mirrors once, with corresponding redshifts.

Recall by the previous calculation that light does not redshift off of the stationary mirror and thus $k_3 = k_2$. This allows us to simply draw a loop diagram labelled with k_1 for the initial momenta and k_2 for the reflected momenta. At first, if we follow what we initially had for interaction vertices on the right and left side of the mirror, the right side given analogously by Eq. 11, then

the amplitude of this diagram for N' interaction vertices on both mirrors would be:

$$iM_1 = \Xi \left(\int \prod_{j=1}^{N'} \left[\frac{d^2k'_j}{(2\pi)^2} \frac{\mathrm{e}^{\frac{i}{2N'}k_1 L}}{(k'_{j+1} - k'_j - i\varepsilon)(k'^2_j - i\varepsilon)} \right] \right)^2 . \tag{46}$$

Here $\Xi = (\mu_L^2 \mu_R^2)^{N'}/2!$. Instead of computing this however, we can use the results we derived for the case of a single loop, analogous to what we had in Eq. 20 and 21. The amplitude for this loop diagram is instead given by:

$$\begin{aligned} iM_1 =& \frac{1}{2!} \int \frac{dk_1}{2\pi} \frac{dk_2}{2\pi} \frac{d^3k}{(2\pi)^3} \frac{\mu_L \mu_R \mathrm{e}^{ik_1 L}}{(k_1^2 + k^2)(k_2^2 + k^2)} \\ &\sim \frac{1}{2!} \int \frac{d^3k}{(2\pi)^3} \frac{\mu_L}{2k_2} \frac{\mu_R}{2k_1} \mathrm{e}^{-2L\sqrt{k^2}} \\ &= \frac{1}{2!} \int \frac{d^3k}{(2\pi)^3} R_L R_R \mathrm{e}^{-2L|k|}. \end{aligned} \tag{47}$$

Now what about the next iteration or reflection? We can write the total contribution to the 1-loop diagram as the sum of loop diagrams at different iterations, labelled similarly to what we had above. This is seen by:

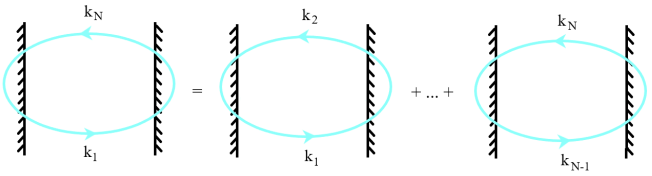

FIG. 18. Contribution of light reflecting off of both mirrors expressed as a sum of 1 loop diagrams for each iteration. It is noted that although the mirrors are drawn to have the same separation, after each iteration the distance increases as $L_j = L + \sum_i^j \delta x_i$.

Adding up all the N contributing diagrams, we are left with the total amplitude integral:

$$iM = \frac{1}{2!} \int \frac{d^3k}{(2\pi)^3} R_L R_R \left[\mathrm{e}^{-2L|k|} + \mathrm{e}^{-2L'|k|} + \dots \right]. \tag{48}$$

We see that in the case of the right mirror moving, we get a sum of exponentials where the arguments of the exponentials have different distances of separation between the mirrors. The second term in the series has $L' = L + \delta x_1 + \delta x_2$. Due to the linearity of integration, we can solve the integrals separately and to recover the force we multiply by a negative sign and differentiate the result with respect to the different cavity separations to get the following:

$$F(L) = \frac{-3 R_L R_R}{16\pi^2} \left[\frac{1}{L^4} + \frac{1}{L'^4} + \dots \right]. \tag{49}$$

This gives us an expression for the force for N reflections without the effects of interference. Once more, to incorporate the effects of the interference of light, we consider a scattering series of diagrams. For each iteration, i.e., each separation of the cavity after a reflection event, we look at many reflections of many photons off of the two mirrors and sum up the contributions. This is similar to what weve done above and is visualized by the diagram sum:

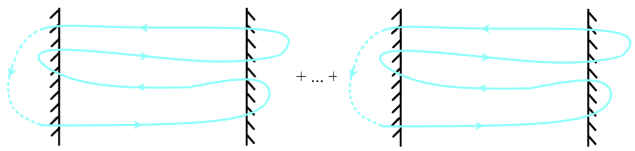

FIG. 19. Contribution of many photons reflecting off of both mirrors for each iteration. Although visually the diagrams only depict four reflections, the diagrams are meant to visualize summing over 1 to N reflections, per iteration, as was done in the static mirror section (which can be thought as the very first iteration only).

As with before, in each iteration, the scattering series changes the integrand to have a logarithmic dependence and results in the expression for the force as:

$$F(L) = \frac{-3\,\mathrm{Li}_4(R_L R_R)}{16\pi^2} \left[\frac{1}{L^4} + \frac{1}{L'^4} + \dots \right]. \tag{50}$$

Now, we would like for the expression to contain velocities only to only have one free parameter, and to better compare with literature results. We first express the different lengths in the denominators as the relative shifts in mirror separations, given by the following:

$$F(L) \sim L^{-4} + \left[L + \sum_{i=1}^{2} \delta x_i \right]^{-4} + \left[L + \sum_{i=1}^{4} \delta x_i \right]^{-4} + \dots \tag{51}$$

Finally, using the results from the beginning of this section, we replace the displacements with the displacement function in terms of velocities and compactly express the form of the force on the mirrors for N reflections, with the effects of interference included:

$$F(v) = \frac{-3\,\mathrm{Li}_4(R_L R_R)}{16\pi^2} \sum_{k=0}^{N/2} \left[L \left(1 + \sum_{i=1}^{2k} v_i \prod_{j=1}^{\lfloor \frac{i-1}{2} \rfloor} \left(\frac{1+v_{2j}}{1-v_{2j}} \right) \right) \right]^{-4}. \tag{52}$$

Now, as expected from the static BCs section, we see the force contributions from interference is suppressed by the L^{-4} factors and when comparing to Eq. 35, the differences in magnitude demonstrates that the interference of light does not pose a problem for photon recycling in a passive cavity. Moreover we give some comments

about the estimated efficiency and acceleration of photon recycling. To calculate the efficiency, we compute the efficiencies $\eta_i = v_{i+1}/v_i$ and average over all the N iterations. This involves recursively plugging in numbers in Mathematica to get the different values of the velocities. It is found that averaging over the efficiencies for $N = 1000$ reflections, we get $\eta \sim 0.513$. Moreover, we compute the force numerically for $N = 1000$ reflections and divide by the mass of the mirror (taken to be $M = 1$ mg or 5.62 GeV in natural units) to get an estimation of the effect of interference on the acceleration of the mirror, noted at δa. It is found that $\delta a \sim 3.36 \times 10^{-22}$ GeV^{-2}.

C. More On Interference

Although in the previous section we saw how interference directly affects the force on the mirror in the context of the DCE, it is interesting to see more explicit descriptions of interference and its relation to a macroscopic force.

1. *Dynamical Casimir Effect*

One approach is to consider a cavity formed by two oscillating Dirichlet mirrors in which the discrete spectrum of created particles in DCE N_k for the k-th mode in an oscillating cavity is [19]:

$$N_k = N_k^L + N_k^R + (-1)^{s+1} 2\sqrt{N_k^L N_k^R}\cos\beta, \tag{53}$$

where N_k^L, N_k^R are the spectrum generated by the left and right mirror, respectively, s is the ratio between the oscillation frequency of the mirror and the fundamental mode frequency φ in the cavity, and β is the phase difference. This looks very similar to the wave intensity I in the case of the double slit interference experiment, given by:

$$I = I_1 + I_2 + 2\sqrt{I_1 I_2}\cos\delta. \tag{54}$$

Here I_i is the intensity of the wave at the ith slit, and δ is the phase difference between the amplitudes. Alternatively, for the case of a moving BC, the positive and negative frequency solutions in the expansion of the scalar field can be put in a vector $\Phi(t, x)$. Moreover, the field can be split in terms of eigenfunction fields on the right and left side of the mirror, denoted by outgoing and incoming fields, respectively. Here in the scattering events of the field with the mirror, causality requires the incoming fields be free and outgoing ones are modified by the interaction with the mirror described as $\Phi_{\text{out}}(\omega) = S(\omega)\Phi_{\text{in}}(\omega)$ [20], for a given frequency ω. It can be shown that applying the scattering procedure to the DCE for small oscillatory, non-relativistic motion, we have corrections for the expression of the outgoing fields:

$$\begin{aligned}\Phi_{\text{out}}(\omega) =& S(\omega)\Phi_{\text{in}}(\omega) + \int \frac{d\Omega}{2\pi}\Phi_{\text{in}}(\Omega)[\delta S_\Omega(\omega,\Omega) \\ &+ q\delta S_q(\omega,\Omega)].\end{aligned} \tag{55}$$

Here δS_i are the corrections to the scattering matrix that are integrated over, and q is the DOF of the mirror. Now, the spectral distribution of created particles can be found by integrating over the trace of the scattering matrix corrections given by:

$$N(\omega) = \int \frac{d\omega'}{2\pi}\frac{\omega}{\omega'}\text{Tr}[\delta S(\omega,-\omega')\delta S^\dagger(\omega,-\omega')], \tag{56}$$

where $\delta S(\omega,-\omega') = \delta S_\Omega(\omega,-\omega') + \delta S_q(\omega,-\omega')$. Here, there are three different contributions to the distribution given by $N(\omega) = N_\gamma(\omega) + N_q(\omega) + N_{\text{int}}(\omega)$. $N_\gamma(\omega)$ represents the spectrum of particles created by a fixed mirror with time dependent properties, $N_q(\omega)$ is the spectrum of particles created by a moving mirror, and $N_{\text{int}}(\omega)$ is the spectrum of particles involved in interference. The component contribution from the interference of the fields is given by:

$$\begin{aligned}N_{\text{int}}(\omega) =& -8\omega\varepsilon^2\tilde{\gamma}_0\tilde{q}_0\int\frac{d\Omega}{2\pi}\frac{1-\gamma_0^2\omega\Omega}{1+\gamma_0^2\Omega^2} \\ &\times 2\text{Re}\{G(\omega+\Omega)F^*(\omega+\Omega)\}.\end{aligned} \tag{57}$$

The prefactor in front of the integral are real constants, while functions F, G are Fourier transforms of source term functions. After computing the integration and normalizing by an affine parameter gives, it can be rewritten in terms of the other contributing term, which takes a very similar form of the interference pattern from the double slit experiment:

$$N_{\text{int}}(\omega) = -\text{sgn}\left[I(\omega)\right] 2\sqrt{N_q(\omega)N_\gamma(\omega)}\cos\phi, \tag{58}$$

where $I(\omega)$ is the intensity amplitude for a given frequency. We see that up to a sign given by the intensity, the spectral distribution of created particles in the DCE is analogous to the intensity distribution of light in the double slit experiment. This shows that the interference of created particles via scalar fields can analogously be interpreted in the same vain as the interference of light.

2. *Electrodynamics*

In the case of electrodynamics, the equations of motion from a Yang-Mills theory reduces to :

$$dF = 0, \quad \star d\star F = J. \tag{59}$$

Here F is the vector bundle-valued curvature two form $F = \frac{1}{2}F_{\mu\nu}dx^\mu \wedge dx^\nu$. Working in local coordinates x^μ of

a chart ϕ, and in the case where we have non-vanishing surface current and charge, we can express them as:

$$\begin{aligned} D^{\mu\nu} &= \frac{\sqrt{-g}}{\mu_0} F^{\mu\nu} - M^{\mu\nu} \\ J^{\mu} &= \partial_\nu D^{\mu\nu},\ f_\mu = F_{\mu\nu} J^\nu. \end{aligned} \tag{60}$$

Here $D^{\mu\nu}$ is an anti-symmetric rank 2 tensor density which includes both the electric displacement field D and the auxiliary magnetic field H. Moreover, $M^{\mu\nu}$ is the magnetization-polarization tensor, and f_μ is the Lorentz force tensor. Using the above and the appropriate BCs, it can be shown that the Lorentz force of two electromagnetic waves at a separating angle θ entering a dielectric medium along the $\hat{z}$-direction with p-polarization is given by [21]:

$$\begin{aligned} F &= -\frac{1}{2}\mathrm{Re}\{J_x B_y^*\} \\ &= 2\pi n \sin\theta/\lambda_0 \left(n^2-1\right)\varepsilon_0 E_0^2 \sin\left(4\pi n x \sin\theta/\lambda_0\right) \\ &= \varepsilon_0 \mathrm{e}_0^2 \left(n^2-1\right). \end{aligned} \tag{61}$$

Here n is the index of refraction of the medium. Without the interference of light and thus the phases of the electromagnetic waves, this quantity would vanish. Taking $n \sim 1.6$ for mirror substrates [22], we get $F \sim 1.56\varepsilon_0 \mathrm{e}_0^2$. Being that the electric permittivity in a vacuum ε_0 is a microscopic quantity and is very small, the force from the interference of light on a mirror in heavily suppressed when compared to the radiation pressure.

IV. BRIEF COMMENTS

Within [4], in addition to claiming that the interference of light will completely cancel out the contribution of radiation pressure on the propulsion of the HR payload, they also claim that the kinetic energy delivered to the spacecraft in a passive cavity without an active gain medium, is less than that by the single reflection of laser sail with the incident laser beam, which we will call the reference energy. In the paper, the kinetic energy gained by the payload is found by integrating over the thrust L:

$$E_p = \frac{2P_{\mathrm{inc}}}{c} \frac{T}{(1-R)^2} \int_{L_0}^{L} \frac{dL}{1 + F_c \sin^2(k'L)}. \tag{62}$$

Here P_{inc} is the incident laser power, T is the transmittance of the cavity, R is the reflectivity of the cavity, $k' = k + \delta_r/2$ is the modified wavenumber of the laser beam with $\delta_r/2$ being the phase difference for one reflection, and F_c is the coefficient of finesses of the cavity. In it, they approximate the above integral to be:

$$E_p \approx \frac{2P_{\mathrm{inc}}}{\pi c}(L - L_0) \tag{63}$$

This is then compared to the reference $E_{\mathrm{ref}} = \frac{2}{c}(L - L_0)$, and it is concluded that the energy gained in a passive cavity is strictly less than the reference energy and thus is impractical. Computing the integration is done with a few trigonometric substitutions and results in:

$$E_p = \left[\frac{TP_{\mathrm{inc}}}{2cR}\right]\left(\frac{\cot(L_0 k') - \cot(Lk')}{k'}\right). \tag{64}$$

The reference energy can be manipulated to be written with the same prefactor above to give:

$$E_{\mathrm{ref}} = \left[\frac{TP_{\mathrm{inc}}}{2cR}\right]\left(\frac{4\sqrt{R}}{\pi(1-R)}\right)(L - L_0). \tag{65}$$

Due to the factor of $1/k'$ in E_p, there will be periodic divergences in $\pm\infty$, so it is not well-defined when the reference energy is higher than the kinetic energy gained in a passive cavity.

Moreover, for an active cavity, once again they approximate the integral for the energy gained in an active cavity with an active gain medium:

$$\begin{aligned} E_a =& \frac{2\varepsilon^2}{P_p c} \int_{L_0}^{L} \frac{dL}{|1 - \exp(\frac{1}{2}(\delta_m - \Delta) - 2ik'L)|^2} \\ &\approx \frac{2\varepsilon^2}{P_p \Delta c}(L - L_0). \end{aligned} \tag{66}$$

Here P_p is the power of the pump laser feeding energy into the active gain medium, η is the pumping efficiency in the amplitude of the gain medium, δ_m is round-trip power gain factor, and Δ is the total round-trip loss factor. After computing the modulus in the denominator, the integral is computed numerically and gives:

$$E_a = \frac{\varepsilon^2 \left[\mathrm{arctanh}(\Gamma \tan(Lk')) - \mathrm{arctanh}(\Gamma \tan(L_0 k'))\right]}{k'\Gamma}. \tag{67}$$

Here $\Gamma = \sqrt{-(1 + 4\exp(1/2(\delta_m - \Delta)))}$. Once again, due to the $1/k'$ factor, the result is periodically divergent, and it is not clear when it is greater than the reference energy. Thus, the claims made against the passive cavity based on comparing it to the reference energy are invalid.

V. CONCLUSION

In this paper we developed a Feynman diagram approach to characterize the effects of light interference on the radiation pressure exerted on a moving mirror. We studied the different quantum effects including interference in the separate cases that the mirrors don't move, and one moves relativistically. We also looked at the effects of the interaction or scattering of light via loop diagrams, and the dynamical Casimir effect. It is found

for the case of scattering, the amplitude is suppressed by factors of the electron mass in the virtual electron loop. Moreover, for the case of interference, the change in radiation pressure is suppressed by factors of L^{-4}, where L is the initial separation of the mirrors in the cavity. It is thus concluded that the effects of interference are negligible for propulsion via photons bouncing in a cavity. Moreover, for $N = 1000$ reflections, it is also found that the efficiency of photon recycling is $\eta \sim 0.513$, and the effect of interference on the acceleration of the mirror is given by $\delta a \sim 3.36 \times 10^{-22}$ GeV^{-2} which is again small compared to the macroscopic acceleration given in cited literature.

VI. ACKNOWLEDGEMENTS

I would like to thank Simon Caron-Huot for the idea and our discussions on describing light reflection and interference as a spatially-dependent interaction vertex in the scalar field theory.

VII. APPENDIX

A. Casimir Force: Functional Determinant Approach

In this section we briefly cover the alternate method used to derive the Lifshiftz formula for the Casimir force using the Gelfand-Yaglom theorem [11].

We consider a fluctuating real scalar field in D+1 spacetime dimensions where the field is coupled by two imperfect, thick mirrors modelled as potentials V_i on their positions. The Euclidean action $S[\varphi] = S_0[\varphi] + S_I[\varphi]$, has the usual free action for scalar fields $S_0[\varphi]$ and an interaction action. The mirrors are parallel to each other along the x_D, while all other directions are denoted as $\bar{x} = x_1, \ldots, x_{D-1}$. We bound the system to reside within a D-dimensional box subject to the same Dirichlet BC on all 2d boundaries, with side lengths $\bar{l}$ for $\bar{x}$ and l for x_D. The setup of the physical system is depicted as follows:

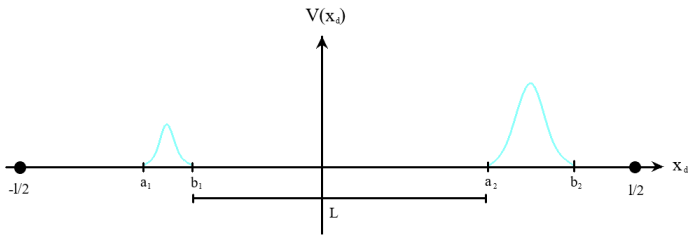

FIG. 20. Physical setup of system with two wide and different potentials modelling the positions and thicknesses of the mirrors.

The interaction between the mirror potentials and the scalar field is given by the action:

$$S_I[\varphi] = \frac{1}{2}\int d^{D+1}x d^{D+1}x' \delta(x_D - x'_D) V(x_D, \bar{x} - \bar{x}') \times \varphi(x)\varphi(x'), \tag{68}$$

where the potential argument in the action is of the form:

$$V(x_D, \bar{x} - \bar{x}') = V_1(x_D - a_1)\lambda_1(\bar{x} - \bar{x}') + V_2(x_D - a_2)\lambda_2(\bar{x} - \bar{x}'). \tag{69}$$

Now, we want to compute the vacuum energy between the mirrors without the contribution of the individual mirror's selfenergy. This is done with the spatial temporal limit:

$$\varepsilon = \frac{1}{2}\lim_{T,\bar{l}\to\infty}\left(\frac{1}{T\bar{l}^{d-1}}\log\frac{Z}{Z_0}\right). \tag{70}$$

Here, Z is referring to the continuous limit of the partition function in real time, expressed as the path integrals over the different field configuration φ:

$$Z = \int \mathcal{D}\varphi e^{-S[\varphi]}, Z_0 \equiv Z|_{V\to 0}. \tag{71}$$

Now, we can write down the exact solution for the partition function by expressing it in terms of a functional determinant:

$$Z = \sqrt{\det[-\partial^2 + m^2 + V]} \equiv \sqrt{\det \chi}. \tag{72}$$

Here, χ acts on variables $x \in R^{D+1}$ which vanish on the boundary on the boundary of the imposed box. We can use separation of variables (SOV) to reduce the problem to deal with operators acting on a univariate variable x_D and momentum $k = (k_0, \ldots, k_{D-1})$ as follows:

$$\det \chi = \prod_k \det \tilde{\chi}(k), \tag{73}$$

where $\tilde{\chi}(k)$ has the form:

$$\tilde{\chi}(k) = -\partial^2 + \Omega^2(k) + \tilde{V}(x_D, k), \;\; \Omega(k) = \sqrt{k^2 + m^2}. \tag{74}$$

Putting this in our expression for the vacuum energy and taking the continuous limit to get integration in D dimensions gives the following form:

$$\varepsilon = \frac{1}{2}\int \frac{d^D k}{(2\pi)^D}\log\left[\frac{\det\tilde{\chi}(k)}{\det\tilde{\chi}_0(k)}\right]. \tag{75}$$

Now, we make use of the Gelfand-Yaglom theorem which relates functional determinants of the one-dimensional second order differential operators to the solutions of the corresponding initial value problem [23]. After shifting and re-scaling coordinates, we express the ratio of the determinants as the ratio of solutions to the associated homogeneous equations:

$$\frac{\det \tilde{\chi}(k)}{\det \tilde{\chi}_0(k)} = \frac{\psi(\frac{l}{2})}{\psi_0(\frac{l}{2})}, \tag{76}$$

where $\psi(x)$ solve the associated homogeneous equations:

$$\tilde{\chi}(k)\psi(x_D) = 0, \quad \tilde{\chi}(k)\psi_0(x_D) = 0. \tag{77}$$

Once again, putting this in our expression for the vacuum energy and differentiating with respect to the length of the box gives:

$$F(L) = \frac{1}{2}\int \frac{d^D k}{(2\pi)^D}\frac{\partial}{\partial L}\log\left[\frac{\psi(\frac{l}{2})}{\psi_0(\frac{l}{2})}\right]. \tag{78}$$

In order to compute $\psi(l/2)$, we rewrite the relations of solutions to the initial value problems with matrices as:

$$\Psi(x_f) = A(x_f, x_i)\Psi(x_i), \tag{79}$$

where $\Psi(x)$ and $A(x)$ have the following forms, respectively:

$$\Psi(x) = \begin{bmatrix} \psi(x) \\ \psi'(x)/\Omega \end{bmatrix}, \; A(x_f, x_i) = U(x_f)U^{-1}(x_i). \tag{80}$$

Here $U(x)$ is the Wronskian matrix made up of independent solutions of the homogeneous equation. A is known as the transfer matrix that allows us to evaluate ψ, ψ' on the right side of each mirror in terms of their values on the left side of the mirrors. The intervals between the mirrors can be split up into portions where the potential vanishes and it can be shown that the transition matrix has the form:

$$\begin{aligned} A(l/2, -l/2) =& A^{(0)}(l/2, b_2)A^{(V_2)}(b_2, a_2)A^{(0)}(a_2, b_1) \\ & \times A^{(V_1)}(b_1, a_1)A^{(0)}(a_1, -l/2). \end{aligned} \tag{81}$$

$A^{(0)}$ can be found using the U_{00} and U_{01} components of the Wronskian matrix that houses the individual solutions. It can then be shown that using the expression for A above that the solutions $\psi(x)$ take the form:

$$\psi(l/2) = u_2^{\mathrm{T}} A^{(2)}A^{(0)}A^{(1)}v_1, \tag{82}$$

where

$$u_i = \begin{bmatrix} \cosh \Omega l_i \\ \sinh \Omega l_i \end{bmatrix}, \; v_i = \begin{bmatrix} \sinh \Omega l_i \\ \cosh \Omega l_i \end{bmatrix}. \tag{83}$$

Finally, the derivative of the logarithm of the solutions ψ is shown to be (in the limit $l \to \infty$):

$$\left[\frac{\partial \log \psi(l/2)}{\partial l}\right]_{l\to\infty} = \frac{\Omega U_{01}(x)\omega_1^{\mathrm{T}} A^{(2)} C A^{(1)}\omega_1}{\omega_1^{\mathrm{T}} A^{(2)}A^{(0)}A^{(1)}\omega_1}. \tag{84}$$

Where $\omega_1 = 1/\sqrt{2}\,(1,1)^{\mathrm{T}}$ and $C = \sigma_x - \mathbb{1}_{2\times 2}$. We can finally rotate to the ω_i where $\omega_2 = 1/\sqrt{2}\,(1,-1)^{\mathrm{T}}$ which in turn affects $A^{(0,1,2)} \to T^{(0,1,2)}$ & $C \to D$. Next, we take the $l/L \to \infty$ limit and expand up to L/l to first order to get the expression:

$$\left[\frac{\partial \log \psi(L/2)}{\partial l}\right]_{\frac{l}{L}\to\infty} = \frac{\partial}{\partial l}\log\left[1 + \frac{T_{12}^{(2)}T_{21}^{(1)}}{T_{11}^{(2)}T_{11}^{(1)}}U_{01}^2\right]. \tag{85}$$

Finally, to get the force per unit volume in terms of the reflection coefficients of the mirrors, we associate $U_{00} = \mathrm{e}^{\Omega x}$ & $U_{01} = \mathrm{e}^{-\Omega x}$ and the quantities $r^{(1)} = \frac{T_{21}^{(1)}}{T_{11}^{(1)}}$ & $r^{(2)} = -\frac{T_{12}^{(2)}}{T_{11}^{(2)}}$ as the reflection coefficients of the left and right mirror, respectively. This gives the final form:

$$F(L) = -\frac{1}{2}\int \frac{d^D k}{(2\pi)^D}\frac{\partial}{\partial L}\log\left[1 - r_R^{(1)}r_L^{(2)}\mathrm{e}^{-2\Omega L}\right]. \tag{86}$$

This is exactly in accordance with the expression we derived using Feynman diagrams, except instead with functional determinants.

[1] Young K. Bae. Photonic Laser Thruster: Optomechanical and Quantum Electronical Analyses. *Journal of Propulsion and Power*, January 2022.

[2] Amnon Yariv. *4 Optical Resonators*. Saunders College Publ., 1991.

[3] Neeraj Kulkarni, Philip Lubin, and Qicheng Zhang. Relativistic Spacecraft Propelled by Directed Energy. *The Astronomical Journal*, 155(4):155, March 2018.

[4] Young K. Bae. Photonic Laser Thruster: 100 Times Scaling-Up and Propulsion Demonstration. *Journal of Propulsion and Power*, 37(3):400–407, May 2021.

[5] Martin H. Weik. *active laser medium.* Springer US, Boston, MA, 2001.

[6] Michael Edward Peskin and Daniel V. Schroeder. *An introduction to quantum field theory.* Addison-Wesley Pub. Co, Reading, Mass, 1995.

[7] Machado. Quantum radiation pressure on a moving mirror at finite temperature. *Physical Review D*, 66(10):105016, November 2002.

[8] Salvatore Butera. Influence functional for two mirrors interacting via radiation pressure. *Physical Review D*, 105(1):016023, January 2022.

[9] Chad R. Galley, Ryan O. Behunin, and B. L. Hu. Oscillator-field model of moving mirrors in quantum optomechanics. *Physical Review A*, 87(4):043832, April 2013.

[10] Michael R R Good. Quantized Scalar Fields Under the Influence of Moving Mirrors and Anisotropic Curved Spacetime. *NA*, page 180, 2011.

[11] C. Ccapa Ttira, C. D. Fosco, and F. D. Mazzitelli. Lifshitz formula for the Casimir force and the Gelfand-Yaglom theorem. *Journal of Physics A: Mathematical and Theoretical*, 44(46):465403, November 2011. arXiv: 1107.2357.

[12] D. F. Walls. A simple field theoretic description of photon interference. *American Journal of Physics*, page 6, 1977.

[13] Masud Mansuripur. Deducing radiation pressure on a submerged mirror from the Doppler shift. *Physical Review A*, 85(2):023807, February 2012.

[14] Yi Liang and Andrzej Czarnecki. Photon–photon scattering: a tutorial. *Canadian Journal of Physics*, 90(1):11–16, January 2012.

[15] Naser Ahmadiniaz, Cristhiam Lopez-Arcos, and Misha A Lopez-Lopez. The QED four – photon amplitudes off-shell: part. *Journal of High Energy Physics*, page 39, 2020.

[16] Danilo T. Alves, Edney R. Granhen, and Mateus G. Lima. Quantum radiation force on a moving mirror with Dirichlet and Neumann boundary conditions for a vacuum, finite temperature, and a coherent state. *Physical Review D*, 77(12):125001, June 2008.

[17] S. A. Fulling and P. C. W. Davies. Radiation from a moving mirror in two dimensional space-time: conformal anomaly. *Proceedings of the Royal Society of London. A. Mathematical and Physical Sciences*, 348(1654):393–414, March 1976.

[18] Yu-Song Cao and Yanxia Liu. Feynman diagram approach to dynamical Casimir effect in optimechanical cavity. *arXiv:2103.10657 [quant-ph]*, October 2021. arXiv: 2103.10657.

[19] Jeong-Young Ji, Hyun-Hee Jung, and Kwang-Sup Soh. Interference phenomena in the photon production between two oscillating walls. *Physical Review A*, 57(6):4952–4955, June 1998.

[20] Jeferson D. Lima Silva, Alessandra N. Braga, Andreson L.C. Rego, and Danilo T. Alves. Interference phenomena in the dynamical Casimir effect for a single mirror with Robin conditions. *Physical Review D*, 92(2):025040, July 2015.

[21] Masud Mansuripur. Radiation pressure and the linear momentum of the electromagnetic field. *Optics Express*, 12(22):5375, 2004.

[22] M K Satheesh Kumar and V P Abdullakutty. Determination of Refractive Index of the Mirror Substrate using laser beam interferometry. *Physics Education*, page 6, 2009.

[23] A. Ossipov. Gelfand-Yaglom formula for functional determinants in higher dimensions. *Journal of Physics A: Mathematical and Theoretical*, 51(49):495201, December 2018. arXiv: 1808.02807.